

Influence of electrical parameters of the micro-arc oxidation mode on the structure and properties of coatings

**V.Subbotina, V.Bilozerov, O.Subbotin, O.Barmin,
S.Hryhorieva, N.Pysarska**

National Technical University "Kharkov Polytechnical Institute",
2 Kyrpychova Str., 61002 Kharkiv, Ukraine

Received May 7, 2022

The influence of different power sources of the micro-arc oxidation process on the peculiarities of structure formation and properties of coatings on aluminum alloy AB formed in alkali-silicate electrolyte in the anode-cathode mode is investigated. It is shown that the pulse technology and the anode-cathode mode make it possible to form coatings containing mainly oxides of the $\alpha\text{-Al}_2\text{O}_3$ type (corundum) with a high growth rate. It has been established that with a small thickness of the oxide layer, the rate of heat removal both to the metal and to the electrolyte is high; this fact promotes the formation of alumina in the form of the $\gamma\text{-Al}_2\text{O}_3$ phase. The energy concentration in the thick oxidizing layer causes the formation of high-temperature modification of $\alpha\text{-Al}_2\text{O}_3$. It is shown that the mechanism of $\alpha\text{-Al}_2\text{O}_3$ formation is determined by two factors: the energy difference in the formation of $\gamma\text{-Al}_2\text{O}_3$ and $\alpha\text{-Al}_2\text{O}_3$ phases, and the polymorphic high-temperature transformation of $\gamma\text{-Al}_2\text{O}_3 \rightarrow \alpha\text{-Al}_2\text{O}_3$ in the high-temperature region of the arc discharge.

Keywords: micro-arc oxidation, sinusoidal and pulsed power supply, energy consumption, coating morphology, phase-structural state, $\gamma\text{-Al}_2\text{O}_3$ and $\alpha\text{-Al}_2\text{O}_3$ phases.

Вплив електричних параметрів режиму мікродугового оксидування на структуру і властивості покріттів. В.В.Субботіна, В.В.Білозеров, О.В.Субботін, О.Є.Бармін, С.В.Григор'єва, Н.В.Писарська

У статті досліджено вплив різних джерел живлення процесу мікродугового оксидування на особливості структуроутворення та властивості покріттів на алюмінієвому сплаві АВ, сформованих у лужно-силікатному електроліті в анодно-катодному режимі. Показано, що при використанні імпульсної технології й анодно-катодного режиму вдається сформувати покріття, що містять переважно оксиди типу $\alpha\text{-Al}_2\text{O}_3$ (корунд) та забезпечується велика швидкість зростання покріття. Виявлено, що при малій товщині оксидного шару більша швидкість тепловідведення як у метал, так і в електроліт сприяє утворенню оксиду алюмінію у формі $\gamma\text{-Al}_2\text{O}_3$ фази. Концентрація енергії в товстому окиснювальному шарі викликає утворення високотемпературної модифікації $\alpha\text{-Al}_2\text{O}_3$. Показано, що механізм утворювання $\alpha\text{-Al}_2\text{O}_3$ визначається дією двох факторів: різницею енергій утворенню $\gamma\text{-Al}_2\text{O}_3$ і $\alpha\text{-Al}_2\text{O}_3$ фаз, а також поліморфним високотемпературним перетворюванням $\gamma\text{-Al}_2\text{O}_3 \rightarrow \alpha\text{-Al}_2\text{O}_3$ у високотемпературній області мікродугового розряду.

1. Introduction

One of the effective ways to modify the surface of valve metals is the method of microarc oxidation (MAO). The transformation of the treated surface material into oxides and chemical compounds provides strengthening of the surface layers and increase their protective properties [1].

Microarc oxidation makes it possible to obtain multifunctional ceramic-like coatings with a unique set of properties. The essence of the method is to use the energy of electric discharges that cause plasma-chemical, thermal and hydrodynamic effects acting simultaneously, although the degree of their impact may be different [1–5].

The structure, composition and properties of oxide layers are determined by the composition of the oxidizing alloy, the composition of the electrolyte, processing time and electrical parameters of the processing mode specified by the power supply [1–8]. Electrical processing modes determine the thermal, temporal and other characteristics of micro-discharges. To implement the MAO process, capacitor or thyristor power supplies and weakly alkaline electrolytes are used [2–5, 8].

In the case of a capacitor power supply and sinusoidal signal, energy losses occur due to electrical reactions and heating of the electrolyte at times when the voltage in the system "part - bath" is lower than the activation voltage of the process. To reduce the energy losses and increase the effective burning time of microarc discharges in the MAO process, it is advisable to change the sinusoidal current shape to a rectangular one [2–5, 9–20]. Changing the shape from sinusoidal to rectangular ultimately reduces energy consumption in the formation of MAO coatings, and should affect the processes of structure formation [2–5].

However, previous works [1–5] do not allow formulating recommendations for controlling the structure and properties of coatings depending on the modes of the technological process. The aim of this work is to study the influence of various power sources in the microarc oxidation (MAO) process on the features of structure formation and the properties of coatings formed in an alkaline-silicate electrolyte in the anode-cathode mode on aluminum alloy AB.

2. Experimental

The study was carried out using aluminum alloy AB samples in an aqueous solution of 1 g/l KOH + 3 g/l Na₂SiO₃ (liquid

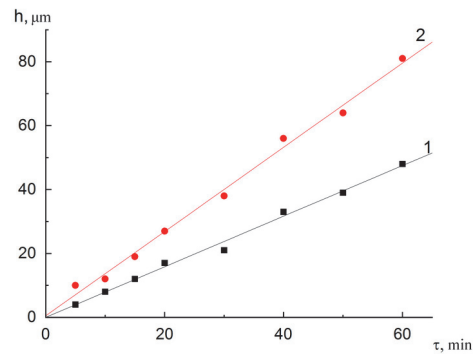


Fig. 1. Kinetics of coating formation over thickness (current density $j \approx 20 \text{ A/dm}^2$, $U_a = 560 \text{ V}$, $U_c = 300 \text{ V}$, $f = 300\text{--}400 \text{ Hz}$); 1 — sinusoidal current; 2 — pulse current.

glass), provided cooling and bubbling of the electrolyte.

The following power sources were used in the process of microarc oxidation:

- power supply from a capacitor-type alternating current (AC) network with a sinusoidal voltage (voltage 380 V, frequency 50 Hz, power 40 kW, ratio of anode and cathode currents $I_a/I_c = 1$;

- thyristor-type switching power supply, consisting of two main units: an adjustable DC source and a power supply. The adjustable DC power supply is a controlled three-phase thyristor rectifier with a capacitor unit capable of adjusting the voltage from zero to nominal. The power unit is a thyristor inventory that allows you to change the pulse duration and frequency, and provide a quasi-rectangular alternating pulse shape.

Switching power supply allows you to independently adjust the amplitude, pulse duration and frequency of positive and negative voltage with the possibility of stabilizing the current amplitude in the microarc processing. Signal pulses with a duty cycle of 120–150μs with a frequency of 60–1400 Hz were used.

The comparative analysis of the kinetics of coating thickness formation, their phase-structural state, properties, energy consumption for sinusoidal and pulsed molding modes was carried out.

3. Results and discussion

The dependence of the coating thickness on the duration of oxidation for different oxidation regimes is shown in Fig. 1.

The linearity of the dependence indicates that the thickness of the coating is propor-

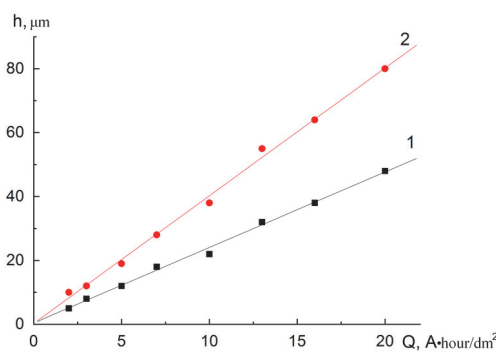


Fig. 2. Dependence of the coating thickness on the amount of energy passed (current density $j \sim 20 \text{ A}/\text{dm}^2$); 1 — sinusoidal current; 2 — pulse current.



Fig. 3. Morphology of the coating surface ($\times 300$).

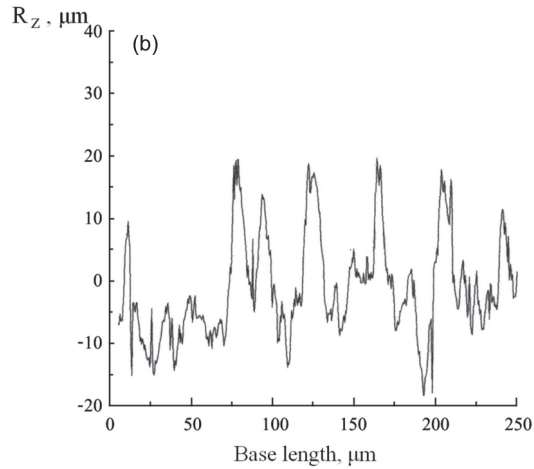
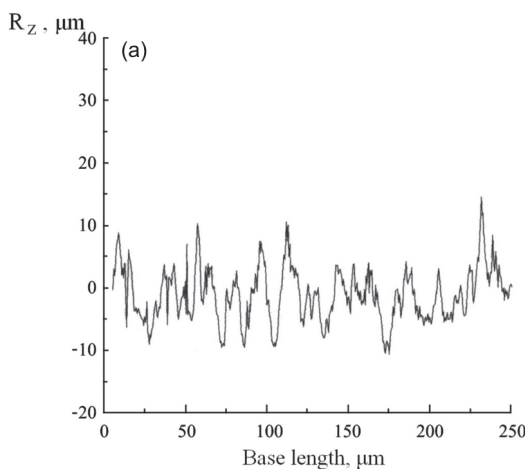


Fig. 4. Surface roughness of coatings ($h_{total} = 50 \mu\text{m}$); a — pulse mode; b — sinusoidal mode.

tional to the amount of electricity passed. However, pulsed technology provides a greater rate of formation of the coating thickness. In the sinusoidal mode, the coating growth rate is $\sim 0.8 \mu\text{m}/\text{min}$, and in the pulse mode, $\sim 1.3 \mu\text{m}/\text{min}$, which significantly affects energy consumption. Thus, if the change in the thickness of the coating is expressed depending on the energy consumed or the amount of electricity passed, then their linear relationship is detected (Fig. 2). Estimation of the energy consumption in the formation of coatings with a thickness of $\sim 100 \mu\text{m}$ showed that the specific energy consumption for the formation of the coating is ~ 14 and $8 \text{ kW}\cdot\text{h}/\text{dm}^2$, respectively, for sinusoidal and pulse modes. Thus, pulse technology can reduce energy consumption by 75 %.

Both sinusoidal and pulse modes result in a highly developed surface morphology

(Fig. 3). At the same coating thickness ($h = 50 \mu\text{m}$) no significant differences were found. However, the surface roughness is different (Fig. 4). This result is due to the different density, mobility, and power of micro-discharges. The high density of discharges in the pulsed mode provides less roughness and stepwise irregularities in the coating.

One of the structural features of coatings is their layered structure. The two-layer structure is revealed metallographically on transverse sections (Fig. 5). The top layer is technological, low-strength, porous, easily removed. The inner layer is working, monolithic, wear-resistant. Its thickness is 60–70 % of the total thickness of the coating.

The two-layer structure of the coatings is characteristic of both sinusoidal and pulsed mode.

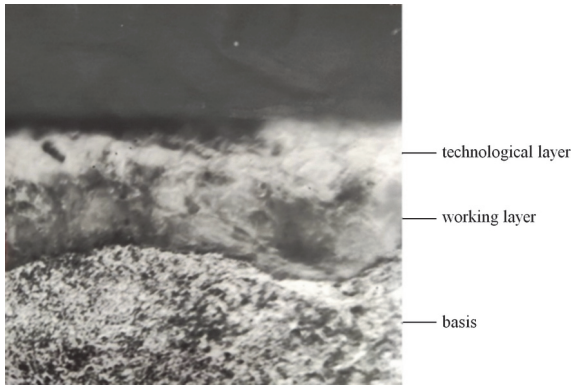


Fig. 5. Microstructure of a coating ($\times 400$) ($h_{total} = 50 \mu\text{m}$).

X-ray phase analysis of the technological layer (Fig. 6) showed that the main phases are mullite ($3\text{Al}_2\text{O}_3 \cdot 2\text{SiO}_2$) and an amorphous phase; $\alpha\text{-Al}_2\text{O}_3$ and $\gamma\text{-Al}_2\text{O}_3$ phases are present in a small amount. The analysis of the diffraction pattern (Fig. 6) gave the following phase composition: 35 % of the amorphous phase, 42 % mullite, 11 % $\alpha\text{-Al}_2\text{O}_3$, 12 % $\gamma\text{-Al}_2\text{O}_3$. The high amount of the amorphous phase and mullite in the coating does not provide wear resistance of the coating. The diffraction pattern of the working layer (Fig. 7) is fundamentally different: no amorphous phase, the main phase is $\alpha\text{-Al}_2\text{O}_3$, traces of mullite and $\gamma\text{-Al}_2\text{O}_3$ are detected (87 % $\alpha\text{-Al}_2\text{O}_3$, 7 % $\gamma\text{-Al}_2\text{O}_3$, 6 % mullite).

Let us note the following features of the phase composition of the working layer in coatings formed in different modes:

1. Sinusoidal mode: with a coating thickness of up to 50 μm , the phase composition is constant and consists of the $\gamma\text{-Al}_2\text{O}_3$ phase. The conditions of polymorphic transformation of $\gamma\text{-Al}_2\text{O}_3 \rightarrow \alpha\text{-Al}_2\text{O}_3$ are not realized. The power of micro-discharges is not enough to ensure the temperature of the polymorphic transformation ($t \sim 1200^\circ\text{C}$).

2. Pulse mode: phase formation starts from the $\gamma\text{-Al}_2\text{O}_3$ phase. At a coating thickness of $\sim 20 \mu\text{m}$, the $\alpha\text{-Al}_2\text{O}_3$ phase appears, i.e. the polymorphic transformation $\gamma \rightarrow \alpha$ occurs. With an increase in the coating thickness, the content of $\alpha\text{-Al}_2\text{O}_3$ phase increases, and at the coating thickness of 50–60 μm , the content exceeds 80 % by weight.

The phase composition of the coating determines their properties. Thus, in the sinusoidal mode, the hardness of the base layer does not exceed 10 GPa, while in the pulsed mode, the hardness reaches 20 GPa

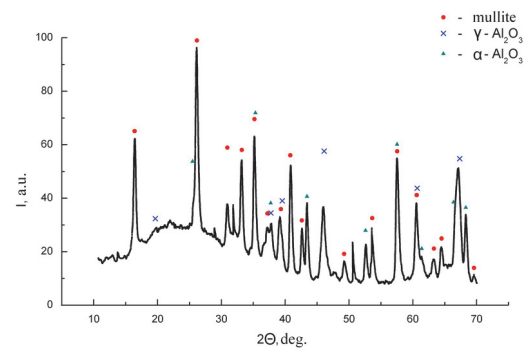


Fig. 6. Diffraction pattern of the technological layer of the coating (Cu-K α radiation).

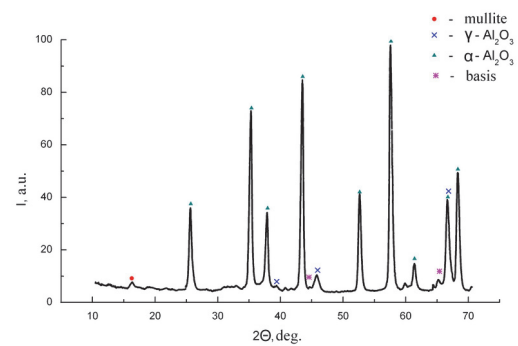


Fig. 7. Diffraction pattern of the working layer of the coating (Cu-K α radiation).

(when the content of $\alpha\text{-Al}_2\text{O}_3$ phase is more than 70 %).

Thus, the use of the pulsed mode makes it possible to significantly change the phase composition of the coatings and, as a consequence, their hardness (Fig. 8).

In order to optimize the modes of pulse processing, the coatings obtained in different modes were studied (Table 1). An analysis of these results shows that at $U_a = 550\text{--}580 \text{ V}$, $U_c = 120\text{--}185 \text{ V}$, $j = 12\text{--}16 \text{ A/dm}^2$ (mode 1–5, see Table 1), there is an extreme dependence of the $\alpha\text{-Al}_2\text{O}_3$ content in the coating and hardness depending on the pulse frequency. The maximum content of $\alpha\text{-Al}_2\text{O}_3$ phase in the coating is provided at $f = 300\text{--}400 \text{ Hz}$, which corresponds to a pulse duration of 2000 μs (Fig. 9).

Regardless of the parameters of the pulse mode MAO (Table 1), the thickness of the coating is determined by the amount of electricity passed (Fig. 10).

Table 1. Parameters of microarc oxidation processing in the pulse mode of molding and properties of the obtained coatings

Regime	High-voltage, V		Current density, A/dm ²	Frequency, Hz	Processing time, τ, min	Specific energy consumption, kWh/dm ²	Coating thickness, h, μm	$C\gamma^+$, Cm, %	C_a , %	HV, GPa
	+	-								
1	580	120	11.9*	60	66	13.1	50	65	35	10.2–10.9
2	550	200	15.7	160	66	15.7	65	47	53	16
3	550	265	14.3	320	64	17.3	70	35	65	17
4	570	270	16.7	600	60	16.7	70	50	50	15
5	550	185	14.3	870	60	14.3	60	55	45	13
6	580	460	23.8	1200	50	19.8	70	32	68	18
7	580	360	38.1	1200	50	31.8	120	50	50	17
8	570	380	26.2	1400	50	21.8	80	28	72	20
9	400	160	25.2	1200	5	2.1	12	100	0	–
10	400	160	25.2	1200	10	4.2	20	100	0	–
11	400	160	25.2	1200	15	6.3	25	100	0	–

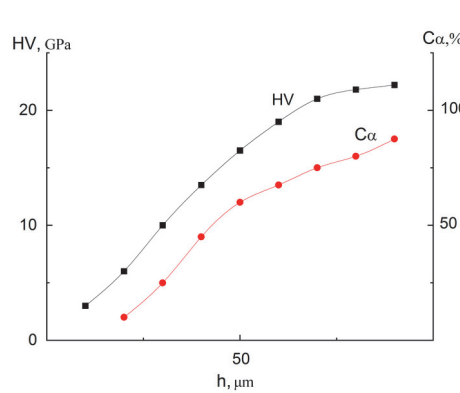


Fig. 8. Phase composition and hardness of coatings (pulse mode).

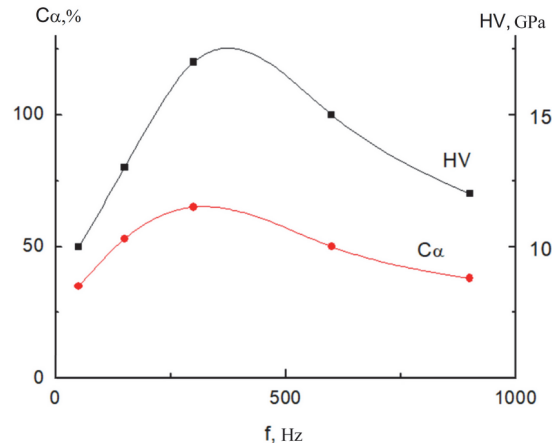


Fig. 9. Phase composition and hardness of coatings depending on the frequency of pulse processing.

4. Conclusions

Micro-arc processing of aluminum alloys in an alkaline-silicate electrolyte using pulsed technology and an anode-cathode mode makes it possible to form coatings containing mainly oxides of the α -Al₂O₃ (corundum) type. A higher density of micro-discharges in pulsed technology increases the total energy released in them, which increases the probability of the formation of the α -Al₂O₃ phase. A linear dependence of the coating thickness on the duration of the process was found, i.e. from the amount of electricity passed. The pulsed technology provides a faster growth rate of the coating. It was found that with a small thickness of the oxide layer, a higher heat removal rate in both the metal and the elec-

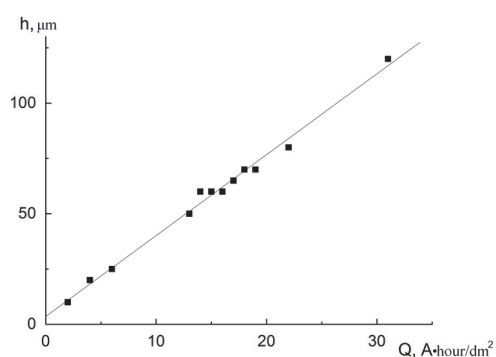


Fig. 10. Dependence of the coating thickness on the amount of electricity passed (different modes of molding, see Table 1).

trolyte promotes the formation of alumina in the form of the γ -Al₂O₃ phase. The concentration of energy in the thick oxidizing layer causes the formation of the high-temperature modification α -Al₂O₃. It is shown that the mechanism of α -Al₂O₃ formation is determined by two factors: the difference in the energies of the γ -Al₂O₃ and α -Al₂O₃ phases, as well as the polymorphic high-temperature transformation of γ -Al₂O₃ \rightarrow α -Al₂O₃ in the high-temperature region of the micro-arc.

References

1. I.V.Sumakov, A.V.Epel'fel'd, V.B.Lyudin et al., *Mikrodugovoe Oksidirovanie* (Teoriya, Tekhnologiya, Oborudovanie), EKOMET, Moscow (2005) [in Russian].
2. I.S.Ponomarev, E.A.Krivonosova, *Sovremennoye Problemy Nauki i Obrazovaniya*, **6**, 135 (2014).
3. F.C.Walsh, C.T.J.Low, R.J.K.Wood et al., *Trans. Inst. Met. Finish.*, **87**, 122 (2009).
4. Zh.M.Ramazanova, L.M.Mustafa, *Materiалovedenie. Kompleksnoe Ispol'zovanie Mineral'nogo Syr'ya*, **3**, 61 (2015).
5. A.K.CHubenko, N.I.Mamaev, Yu.Yu.Beznickaya, T.I.Dorofeeva, *Nauchno-tehnicheskij Vestnik Povolzh'ya*, **2**, 62 (2018).
6. E.Matykina, A.Arrabal, P.Skeldon, G.E.Thompson, *Electrochim.Acta*, **54**, 6767 (2009).
7. V.Belozerov, O.Sobol, A.Mahatilova et al., *Eastern-european Journal of Enterprise Technologies*, **91**, 43 (2018).
8. V.Subbotina, U.F.Al-Qawabeha, V.Belozerov et al., *Eastern-european Journal of Enterprise Technologies*, **102**, 6 (2019).
9. P.X.Lv, G.X.Chi, D.B.Wei, S.C.Di, *Advanced Materials Research*, **189–193**, 1296 (2011).
10. C.S.Dunleavy, J.A.Curran, T.W.Clyne, *Surface and Coatings Technology*, **206**, 1051 (2011).
11. M.Javidi, H.Fadaee, *Applied Surface Science*, **286**, 212 (2013).
12. B.W.Zhu, S.Seifeddine, P.O.A.Persson et al., *Materials & Design*, **101**, 254 (2016).
13. R.Prins, *Angewandte Chemie*, **131**, 15694 (2019).
14. W.Yang, Q.Li, W.Liu et al., *Vacuum*, **144**, 207 (2017).
15. S.He, Y.Ma, H.Ye et al., *Corros. Sci.*, **122**, 108 (2017).
16. X.Nie, E.I.Meletis, J.C.Jiang et al., *Surf. Coat. Technol.*, **149**, 245 (2002).
17. Y.O.Oh, J.I.Mun, J.W.Kim, *Surf. Coat. Technol.*, **240**, 141 (2009).
18. K.Tillous, T.Toll-Duchanoy, E.Bauer-Grosse et al., *Surf. Coat. Technol.*, **203**, 2969 (2009).
19. T.W.Clyne, S.C.Troughton, *Int. Mater. Rev.*, **64**, 127 (2018).
20. M.Sieber, F.Simchen, R.Morgenstern et al., *Metals*, **5**, 365 (2018).